ISSN 1870-4069

# Handcraft and Automatic Approaches for the Recognition of Leukemia Images

Rocio Ochoa-Montiel[1,2], Leonardo Martínez Ibarra[3], Humberto Sossa[1,4], Gustavo Olague[5]

[1] Instituto Politécnico Nacional,
Centro de Investigación en Computación,
Mexico

[2] Universidad Autónoma de Tlaxcala,
Facultad de Ciencias Básicas, Ingeniería y Tecnología.
Mexico

[3] Instituto Politécnico Nacional,
Unidad Interdisciplinaria en Ingeniería y Tecnologías Avanzadas,
Mexico

[4] Tecnológico de Monterrey,
Escuela de Ingeniería y Ciencias.
Mexico

[5] CICESE Research Center,
EvoVision Laboratory Ensenada,
Mexico

{ma.rocio.ochoa,humbertososssa,gustavo.olague}@gmail.com,
leonardo.mtz96@outlook.es

**Abstract.** In this paper, we analyze how handcraft and automatic approaches frequently can be used in the recognition of leukemia images. The visual recognition of subtypes of leukemia cells is a difficult problem in medical area. For this reason, the visual analysis is a feasible option when advanced techniques for diagnosis are not available. Additionally, the problem of determining a logic sequence of the process of recognition is equal or more important that the solution itself, which implies to know the advantages and drawbacks of the available approaches to solve a particular problem of visual recognition. Thus, in this paper we present two approaches that allow us become aware of the use of particular techniques in problems such as leukemia cell recognition.

**Keywords:** Machine Vision, Image Recognition, Leukemia Cells.

# 1 Introduction

Leukemia is type of malignant illness that represents one of the main causes of dead in people less than 15 years. Studies suggest that the incidence of a specific leukemia type named Acute Lymphoblastic (AL) in countries like Mexico is among the highest in the world [1]. Although advanced methods exists for detection of this illness, these are very expensive and inaccessible for the most of affected people. Typically, the centers where these methods are available are located in big cities, which increases the cost and time of detection and treatment. For these reasons is a common practice to carry out a visual analysis of blood smears to detect some abnormalities in blood cells, like in leukemia.

On the other hand, an important problem in blood cells recognition is the inherent subjectivity at visual identification of abnormal cells. This is due to factors such as the lack of experience of clinical personal, variability in the smears preparation, or the physical conditions of people who realize the analysis, to mention a few. From the above discussion, it is worth mentioning that a method is needed for doing an adequate recognition of blood cells which minimizes the differences in the observations from different medical specialists and allow us to obtain more accurate diagnosis.

In this regard, the problem of blood cell recognition has been addressed using handcraft approaches [2, 3, 4, 5], where standard techniques of image processing and machine learning are used. Particularly, these techniques use color spaces like CIELab and YUV, morphologic operators and classifiers as k-means and SVM or variations of them. The same problem can be treated with last generation artificial neural networks (ANNs) to automatically extract features and perform classification [6]. These models do not need a previous image processing or explicit feature extraction. Instead they use the image to find adequate descriptors for image classification. Although these models reach adequate results, the process to obtain the features and their meaning is hidden to the user, whereby they are considered black box models. Moreover, they require a lot of computational resources and a great amount of images with medium or low resolution.

## 1.1 Research Contribution

An important contribution of this work is the comparison between handcraft and automatic approaches to address the problem of recognition of leukemia images.

Since in the problem of leukemia cell recognition it is of utmost importance to know how the features are derived in a natural way, as well as their meaning and their importance for the recognition task, the analysis shown in this paper is useful to depict the advantages and drawbacks of handcraft and automatic approaches to solve the recognition particular problem of this paper.

The remainder of this paper is organized as follows. Section 2 describes the materials and the methods used. Section 3 presents the experiments and the results obtained through this research. Finally, Section 4 provides the conclusions.

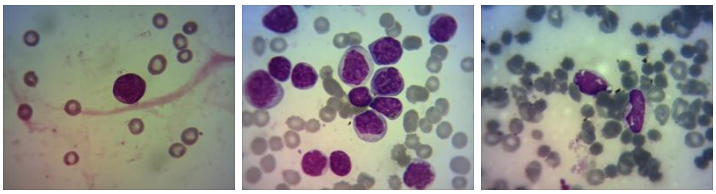

(a) L1 (b) L2 (c) L3

**Fig. 1.** Types of lymphocytic leukemia cells.

## 2 Materials and Methods

In visual analysis of blood white cells, an important criterion for pathology recognition in blood tissue is the cell nucleus, as in leukemia [7]. In blood smears, the nucleus appears as a prominent region of dark purple hues into the cell. Typically, the nuclear features are similar for a specific subtype of blood cell. Fig. 1 shows images of three subtypes of leukemia. Notice that the region of nucleus is particularly different for each one of these subtypes. From this, in this work the nucleus region is used particularly to assessment handcraft techniques for the recognition of leukemia images.

This work is divided into two parts, both carried out independently. A part addresses the use of handcraft approaches, the other part includes tests with automatic approaches. In the former, we use standard image processing techniques to obtain the region of nucleus from the input image. We then consider properties of shape and color from extracted region taking into account the criteria of medical area to recognize these subtypes of cells. Later, the obtained descriptors are feed to two standard classifiers for the recognition of leukemia cells. The second part of the work uses as automatic approaches the convolutional neural networks.

We used a dataset composed by 651 bone marrow smear image from three subtypes of leukemia: L1, L2 and L3, 217 images per class in which expert hematologist provide the classification. Images are in BMP format in color with a resolution of $1280 \times 1024$ pixels. Image acquisition was done by means a Luzeren XSZ-148S optical microscopic with a magnification of 1250 times and a camera coupled to the microscope with a resolution of 1.3 megapixels. For this work, images were resized to $256 \times 320$ pixels using bicubic interpolation. According the subtype of leukemia, the image contains one or more cells of interest as in Fig. 1.

### 2.1 Handcraft Approach

Visual properties of blood cells suggested from literature focused to hematological diseases are considered in this work [7]. Particularly, nucleus traits as shape, color and the distribution of some elements into it are meaningful for cell recognition. From this, the aim in this stage is to extract the nucleus of the bone marrow smear image to obtain adequate descriptors for the recognition of three subtypes of leukemia, L1, L2 and L3.

**Selection of Nucleus.** Since color is a prominent feature to identify the nucleus in images, we use saturation from the HSI color space [8] to obtain an image Is, in which the nucleus is highlighted from the background. Later, a contrast enhancement using a

square function $I_s^2/255$ emphasizes the regions of nucleus preserving its appearance and fading some not useful areas in the image. To select this function, we tried other functions such as inverse, cubic, square root [9]; however, in the output image the region of interest was not properly highlighted.

Output image from the previous step is thresholded by means of Otsu's Method [10]. To remove the remainder noise two criteria are proposed, the area and the Hue (from HSI color space) of nucleus. The first criterion is suggested since the area size of nucleus is typically greater than 200 pixels, this value is obtained by experimentation. Hence, those regions with an area $< 200$ are removed from image.

It is worth noting that this value is applicable to images with a resolution of $256 \times 320$ pixels. Additionally, Hue is useful to discard those pixels that are not removed with the first criteria. Thus, a threshold $T$ is proposed in a range $250 < T < 350$. These thresholds are obtained from the minimum and maximum values founded in the component Hue from nucleous in color images. As a result of applying the last process to each image in dataset, the output binary images contains the regions of the cell nucleus.

**Features extraction.** The selection of features is based on the morphologic traits given by the World Health Organization (WHO) Classification of Tumors and Lymphid Tissues, for the leukemia classification [7]. According to this classification, important properties to identify types of leukemia cells are the size, color, shape and composition of nucleus. Thus, we propose two sets of features *ReducF* and *FullF* to measure these properties, see Tables 1 and 2.

To measure these kind of properties, function *regionsprops* from Matlab Toolbox of Image processing is used. In last phase of the handcraft approach, both sets of features are used to feed two classifiers commonly used for the recognition of the images: a Multi-layer Perceptron (MLP) and Random forest (RF) [12]. The experiments are independently carried out by each classifier.

### 2.2 Automatic Approach

We select two classical convolutional neural network to test the automatic approaches for the cell recognition. LeNet and AlexNet models realize feature extraction and classification automatically from images. In both models, the learning occurs by using the position of patterns directly from the input image data exclusively, without considering previous knowledge about the image. LeNet is a standard CNN [13], while AlexNet [14] use transfer learning. The input is a color image for both nets.

The LeNet architecture used is composed by four sets of convolutional and pooling layers, followed by a flattening convolutional layer, two fully-connected layers, and a softmax classifier. The fully connected softmax output layer produces three possible values that correspond to each class.

AlexNet is a pre-trained net that is eight layers deep and requires an image input size of 227 by 227 by 3, where 3 is the number of color channels. Because the last three layers of the net are configured originally for 1000 classes, these layers are fined-tuned for our problem of classification, replacing them with a fully connected layer, a softmax layer, and a classification output layer.

**Table 1.** *ReducF* Features.

| Number of Feature | Name | Description |
|---|---|---|
| 1 | Num. cells | Number of nucleus in image |
| 2 | Ratio of occupied area | Area Nucleolus / area Cell |
| 3 | Circularity | Ratio of circularity |
| 4 | Euler number | Euler number |
| 5 | Hue | Average of Hue |
| 6 − 12 | Hu's 7 invariants moments | Hu's moments [11] |

**Table 2.** *FullF* Features.

| Number of Feature | Name | Description |
|---|---|---|
| 1 – 12 | Features 1-12 from Table 1 Area | -Number of pixels in nucleus |
| 13 | | |
| 14 | Convex area | Number of pixels in 'ConvexImage' |
| 15 | Eccentricity | Distance between the ellipse foci/major axis length |
| 16 | EquivDiameter | Diameter of a circle with the same area as the region |
| 17 | Extent | Area of the bounding box. |
| 18 | Perimeter | Distance around the boundary of the region |
| 19 | Solidity | *Area/ConvexArea* |
| 20 | Saturation (from HSI) | Average of S |
| 21 | M (fromCMYK) | Average of M |

## 3 Experimental Results

Experiments were executed on a CPU from Intel Core i9- 7900X CPU 3.31Ghz, 64GB RAM, 222Gb hard drive, 64-bit Windows10 Enterprise Edition operating system, graphics processing unit (GPU) GeForceGTX 1080, and MATLAB R2018a.

To address the problem of recognition of leukemia images, first we use a handcraft approach. Thus, to obtain the region of nucleus in the images the process described in section 2.1 is applied.

Then, using the saturation Is from the HSI color space and a contrast enhancement through a square function Is 2/255, the regions of nucleus are emphasized and some regions not useful in the image are dimmed.

The remainder noise from last step is removed using a thresholding with Otsu's Method and a manual thresholding in the component H from HSI image. In this last, the range of hue H for the nucleus region is obtained considering that the minimum and maximum values found in the component Hue from nucleus in color images are in a range of $250 < T < 350$, hence these values are used for the manual thresholding. Fig. 2 shows the result of this processing for an image of leukemia L2.

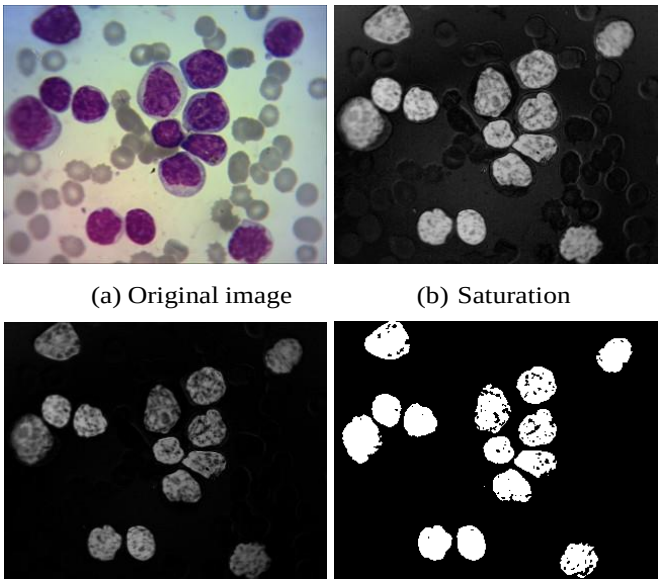

(a) Original image (b) Saturation

(c) Square function (d) Binarized image

**Fig. 2.** First preprocessing sequence for an image of leukemia L2.

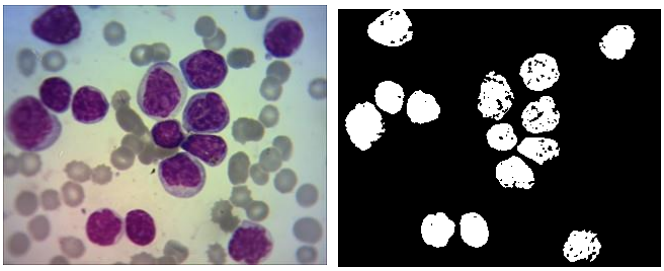

(a) Original image (b) Binary image

**Fig. 3.** Images with extracted nucleus region.

Finally, to eliminate the small regions that remain after thresholding, those regions whose area is less than 200 pixels are removed. This criterion is suggested because the area of nucleus is typically greater than 200 pixels, which was determined with a visual and statistical analysis of the images.

Considering that the images were resized to $256 \times 320$ pixels, the value of area size should be adjusted if images have a different resolution. As a result of applying last process to each image in dataset, the output binary images contain only the regions of the cell nucleus, see Fig. 3.

The binary image obtained in previous stage is used to extract the sets of features proposed in Tables 1 and 2. It is worth mentioning that features 1 and 2 from Table 1 are computed for the full image, while the remainder are obtained calculating the average from the corresponding feature for each region into the image. Most of the

**Table 3.** Results of classification accuracy from 30 executions using MLP

| Set ***ReducF*** | | | | ***Set FullF*** | | | |
|---|---|---|---|---|---|---|---|
| Statistics | Acc-Val | Acc-Test | Time (s) | Statistics | Acc-Val | Acc-Test | Time (s) |
| Without normalizing | | | | | | | |
| Min | 95.35 | 92.82 | 0.44 | Min | 95.35 | 92.31 | 0.47 |
| Max | 99.22 | 97.44 | 2.68 | Max | 100.00 | 97.95 | 5.86 |
| Std | 1.11 | 1.03 | 0.40 | Std | 1.37 | 1.47 | 0.97 |
| Avg | 97.36 | 96.03 | 0.56 | Avg | 97.93 | 96.21 | 0.73 |
| Normalization minmax | | | | | | | |
| Min | 89.92 | 91.28 | 0.44 | Min | 93.80 | 93.33 | 0.47 |
| Max | 97.67 | 96.92 | 2.70 | Max | 100.00 | 97.95 | 2.99 |
| Std | 1.59 | 1.18 | 0.40 | Std | 1.35 | 0.92 | 0.45 |
| Avg | 95.92 | 95.61 | 0.56 | Avg | 98.24 | 96.46 | 0.63 |
| Normalization Zscore | | | | | | | |
| Min | 95.35 | 94.36 | 0.45 | Min | 95.35 | 94.36 | 0.50 |
| Max | 99.22 | 97.44 | 2.71 | Max | 100.00 | 98.46 | 2.84 |
| Std | 1.03 | 0.79 | 0.41 | Std | 1.09 | 0.81 | 0.42 |
| Avg | 97.49 | **96.09** | 0.58 | Avg | 98.27 | **96.82** | 0.63 |

features were obtained using function regions props from the Toolbox of Image processing of Matlab. In all experiments, we used 50% of data for training, 20% for validation and 30% for testing. To valid the classification is used k-FCV (k- Fold Cross Validation) with $k = 5$, and each experiment is carried out 30 times.

The two sets of features are used separately to compare the performance between both groups. Additionally, the experiments consider two types of normalization: minmax and Zscore, and two classifiers: MLP and Random forest. Thus, for each set of features we have three experiments with each classifier, this is using features without normalizing, features normalized with minmax, and features normalized with Zscore. Tables 3 and 4 show the results for these experiments, where is worth to note that normalization Zscore and a set greater of feature is useful in the most of cases. The time for all experiments is low and they do not require a great computing power.

On the other hand, convolutional neural networks LeNet and AlexNet are used as automatic approach. To prevent overfitting, we use image data augmentation including transformations of reflection XY. The input for the nets are the original images in RGB. Accuracy classification we use is the ratio of number of correct predictions to the total number of input examples. This manner, the average of accuracy for testing is 98.36% for LeNet, and 99.98% for AlexNet, however the time is considerably upper to that used by the handcraft approach. This is 188.47 secs. for LeNet, and 836.76 secs. for AlexNet.

Finally, it is important to mention that in the case of the handcraft approach, the visual identification of the leukemia cells could not be clear when the images are similar for the three classes of leukemia as illustrates the Fig. 4. This is because the considered

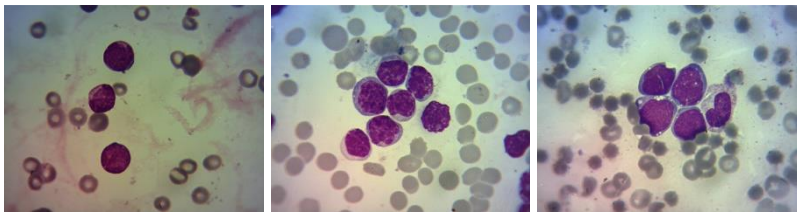

(a) L1 (b) L2 (c) L3

**Fig. 4.** Types of leukemia cells visually similar.

**Table 4.** Results of classification accuracy from 30 executions using Random forest

| **Set *ReducF*** | | | | ***Set FullF*** | | | |
|---|---|---|---|---|---|---|---|
| Statistics | Acc-Val | Acc-Test | Time (s) | Statistics | Acc-Val | Acc-Test | Time (s) |
| Without normalizing | | | | | | | |
| Min | 97.67 | 94.36 | 5.89 | Min | 96.90 | 95.38 | 6.08 |
| Max | 98.45 | 97.44 | 8.52 | Max | 98.45 | 97.95 | 8.75 |
| Std | 0.38 | 0.69 | 0.59 | Std | 0.25 | 0.78 | 0.59 |
| Avg | 97.96 | 95.81 | 6.28 | Avg | 97.67 | **97.08** | 6.75 |
| Normalization minmax | | | | | | | |
| Min | 97.67 | 94.36 | 5.88 | Min | 96.9 | 93.85 | 6.11 |
| Max | 98.45 | 96.92 | 8.65 | Max | 99.22 | 98.46 | 8.80 |
| Std | 0.32 | 0.66 | 0.62 | Std | 0.40 | 1.01 | 0.62 |
| Avg | 97.83 | 95.78 | 6.25 | Avg | 97.62 | 96.77 | 6.42 |
| Normalization Zscore | | | | | | | |
| Min | 97.67 | 94.87 | 5.94 | Min | 96.90 | 95.90 | 6.10 |
| Max | 98.45 | 97.44 | 8.64 | Max | 98.45 | 98.46 | 8.83 |
| Std | 0.39 | 0.66 | 0.61 | Std | 0.52 | 0.61 | 0.60 |
| Avg | 98.06 | **96.19** | 6.29 | Avg | 97.70 | 97.04 | 6.47 |

features are related to the number, morphology and distribution of cells of interest into the image.

Hence, considering that the dataset contains very few cases of this type (approximately 1%), the handcraft approach is useful in part because the RNA learns the patterns of the features derived from the expert knowledge available in the medical area [7].

## 4 Conclusions

This work shows an analysis of the handcraft techniques and automatic techniques for the recognition of leukemia images. It is to note in experiments that although both techniques types offer adequate solutions to the problem of recognition of leukemia

images, handcraft techniques provide explainable knowledge of the way to select the useful features and the logical process to solve the problem.
Instead, using the automatic techniques is not possible to know the way to derive the salient features for addressing the problem of recognition of leukemia images.

In the handcraft techniques, the canonical methods of image processing generated the descriptors that feed to classifiers MLP and random forest for the recognition of cells. This implies that the feature extraction is driven by the human reasoning for the task of recognition of leukemia cells.

On the other hand, results of automatic techniques are competitive, however the process to generate the predictions of model is hidden, which is a notable drawback of these models. Additionally, exist serious limitations regard the image size and the hardware resources required to prove these models.

In brief, the handcraft techniques can provide useful issues for the development of models more robust and explainable learning techniques.

In future work, we would like to use of expert knowledge and symbolic learning to address the problem of recognition of leukemia images.

**Acknowledgements.** This research was supported in part by the Instituto Politécnico Nacional, Mexico under project 20200630. Rocio Ochoa thanks the Autonomous University of Tlaxcala, Mexico for the support. Leonardo Martínez thanks the Delfín program for the economic support to undertake his research stay. All authors thank the Applied Computational Intelligence Network (RedICA).

**Referencias**

1. Colunga-Pedraza, P., Gomez-Cruz, G., Colunga-Pedraza, J., Ruiz-Argüelles, G.: Geographic hematology: Some observations in Mexico. Acta Haematológica, 140, pp. 114–120 (2018)
2. Acharya, V., Kumar, P.: Detection of acute lymphoblastic leukemia using image segmentation and data mining algorithms. Medical and Biological Engineering and Computing, 57, pp. 1783–1811 (2019)
3. Rege, M.V., Gawali, B.W.: Performance evaluation of image segmentation process for recognition of leukemia. In S.S.A.J., eds.: Information and Communication Technology for Intelligent Systems. 107, Springer, pp. 499–509 (2018)
4. Uslu, F., Icoz, K., Tasdemir, K., Yilmaz, B.: Automated quantification of immuno-magnetic beads and leukemia cells from optical microscope images. Biomedical Signal Processing and Control, 49, pp. 473–482 (2019)
5. Negm, A.S., Hassan, O.A., Kandil, A.H.: A decision support system for acute leukaemia classification based on digital microscopic images. Alexandria Engineering Journal, 57(4), pp. 2319 – 2332 (2018)
6. Vogado, L.E.S., Veras, R.M.S., Araujo, F.H.D., Silva, R.R.V., Aires, K.R.T.: Leukemia diagnosis in blood slides using transfer learning in CNNs and SVM for classification. Engineering Applications of Artificial Intelligence, 72, pp. 415–422 (2018)
7. Rodak, B., Carr, J.: Clinical Hematology Atlas. Elsevier (2016)
8. González, R.C., Woods, R.E.: Digital Image Processing. Prentice Hall (2007)

9. De La Escalera, A.: Visión por computador. Fundamentos y métodos (2001)
10. Otsu, N.: A threshold selection method from gray-level histograms. IEEE Transactions on Systems, Man, and Cybernetics, 9(1), pp. 62–66 (1979)
11. Hu, M.K.: Visual pattern recognition by moment invariants. IRE Trans. Information Theory, 8, pp.179–187 (1962)
12. Breiman, L.: Random forest. Machine learning. 45(1), pp. 5–32 (2001)
13. Lecun, Y., Bottou, L., Bengio, Y., Haffner, P.: Gradient-based learning applied to document recognition. Proceedings of the IEEE, 86(11), pp. 2278–2324 (1998)
14. Krizhevsky, A., Sutskever, I., Hinton, G.: Imagenet classification with deep convolutional neural networks. Neural Information Processing Systems, 25 (2012)